A Combined Experimental and Quantum Chemistry Study of Selenium Chemical Shift Tensors

Bryan A. Demko, Klaus Eichele, and Roderick E. Wasylishen*

Department of Chemistry, Gunning/Lemieux Chemistry Centre, University of Alberta, Edmonton, AB, T6G 2G2 Canada

Received: July 18, 2006; In Final Form: September 22, 2006

A comprehensive investigation of selenium chemical shift tensors is presented. Experimentally determined chemical shift tensors were obtained from solid-state ^{77}Se NMR spectra for several organic, organometallic, or inorganic selenium-containing compounds. The first reported indirect spin−spin coupling between selenium and chlorine is observed for Ph_2SeCl_2 where $^1J(^{77}Se,^{35}Cl)_{iso}$ is 110 Hz. Selenium magnetic shielding tensors were calculated for all of the molecules investigated using zeroth-order regular approximation density functional theory, ZORA DFT. The computations provide the orientations of the chemical shift tensors, as well as a test of the theory for calculating the magnetic shielding interaction for heavier elements. The ZORA DFT calculations were performed with nonrelativistic, scalar relativistic, and scalar with spin−orbit relativistic levels of theory. Relativistic contributions to the magnetic shielding tensor were found to be significant for $(NH_4)_2WSe_4$ and of less importance for organoselenium, organophosphine selenide, and inorganic selenium compounds containing lighter elements.

Introduction

Selenium is playing an increasingly important role in chemistry, particularly in materials chemistry. For example, selenium has been utilized in the structure of various nanoparticles, nanowires, and nanotubules.[1−4] Applications have also been reported where selenium is incorporated within the channels of porous materials.[5−10] Interest in selenium chemistry has not seen such growth since it was recognized that selenium is an essential nutrient in mammalian systems.[11] The discovery that the TGA codon directs the incorporation of selenium has ultimately led to the acceptance of selenocysteine as the 21st amino acid.[12,13]

Nuclear magnetic resonance (NMR) has been utilized to investigate a limited number of selenium-containing nanocomposites;[14−17] however, fewer studies have focused on the selenium nucleus itself.[16,17] Selenium-77 NMR is an ideal technique for investigating selenium-containing materials as the ^{77}Se chemical shift ranges over 3000 ppm[18,19] and is extremely sensitive to changes in molecular structure. Clearly, it is desirable to have a sound understanding of the structural features that influence ^{77}Se NMR parameters.

Theoretical calculation of NMR parameters, particularly for selenium where empirical interpretations are more difficult than those extracted from ^{1}H or ^{13}C NMR spectra, has become increasingly useful for spectroscopists.[20] Selenium-77 NMR studies of isotropic liquids, specifically isotropic chemical shifts and indirect spin−spin coupling constants, are a well-developed area of research.[18,19,21−24] The comparison of calculated isotropic chemical shifts with experimental values has recently been criticized as a poor method for determining the accuracy of a given quantum chemical approach given that the fundamental parameter, the magnetic shielding interaction, is characterized by a second-rank tensor containing nine components in general versus the single value obtained from NMR studies of isotropic solutions.[25] Solid-state NMR, which can yield the symmetric part of the chemical shift tensor, is potentially more informative than its solution counterpart;[26,27] however, the literature and scope of solid-state ^{77}Se NMR investigations has been relatively limited.[18,19] Magnetic resonance experiments on heavier nuclei are known to present challenges both experimentally and theoretically,[28] and the question of whether relativistic effects are important for the calculation of ^{77}Se NMR parameters remains a topic of some debate.[28−41]

The aim of the present investigation is to probe a wide variety of selenium-containing solid compounds, covering the known isotropic chemical shift range of selenium, using solid-state NMR spectroscopy and computational chemistry. Specifically, we have used solid-state ^{77}Se NMR spectroscopy to provide the principal components of the chemical shift tensor for several organic, organophosphorus, and inorganic selenium compounds. Because of the inherent ability and success of density functional theory (DFT) in addressing electron correlation, which allows the investigation of larger systems or those containing heavy atoms, DFT was employed to calculate the corresponding selenium magnetic shielding tensors. The DFT calculations were performed at varying levels of inclusion of both scalar and spin−orbit relativistic effects via the zeroth-order regular approximation (ZORA) formalism.[42−45] The calculated magnetic shielding tensors obtained when transformed into chemical shift tensors and compared with the experimental values allow insight into the level of relativistic theory required to accurately describe the observed magnetic shielding.

Background Theory

The magnetic shielding experienced by a nucleus in a molecule generally depends on the orientation of that molecule with respect to the external magnetic field, $\mathbf{B}_0$. This results from induced magnetic fields about the nucleus because of the circulation of electrons, which slightly alter the NMR resonance

* Author to whom correspondence should be addressed. Phone: 780-492-4336. Fax: 780-492-8231. E-mail: roderick.wasylishen@ualberta.ca.

10.1021/jp064543s CCC: $33.50
Published on Web 11/23/2006

condition. To completely describe this shielding, a second-rank tensor, containing up to nine unique components, may be required. In the magnetic shielding tensor's principal axis system (PAS), the symmetric part of the tensor is diagonal, and only three orthogonal components ($\sigma_{11} \leq \sigma_{22} \leq \sigma_{33}$), and three Euler angles (α, β, γ), which relate the orientation of the PAS to the molecular frame, are required to properly describe the interaction tensor. The span of the shielding tensor is defined as $\Omega = \sigma_{33} - \sigma_{11}$ and represents the maximum orientation dependence of the shielding experienced by the nucleus in a given molecule. The isotropic shielding, σ_{iso}, is one-third the trace of the shielding tensor, $\sigma_{iso} = (\sigma_{11} + \sigma_{22} + \sigma_{33})/3$. The NMR spectrum of a powdered sample containing an "isolated spin" yields the principal components of the chemical shift tensor, whose values are related to the magnetic shielding tensor by

$$\delta_{ii}(\text{sample}) = \frac{\sigma_{iso}(\text{ref}) - \sigma_{ii}(\text{sample})}{1 - \sigma_{iso}(\text{ref})} \quad (1)$$

where σ_{iso}(ref) is the isotropic shielding of a standard reference and $\delta_{11} \geq \delta_{22} \geq \delta_{33}$. Solid-state NMR can also provide the Euler angles; however, single crystals of sufficient size and quality are usually required for their determination,[46−50] and as a consequence, Euler angles are less commonly reported than the principal components which are readily obtained from powdered samples.

The nonrelativistic theory of nuclear magnetic shielding was developed by Ramsey[51,52] and is recognized as among the most influential papers in 20th century quantum chemistry.[53] The significance of relativistic effects in the calculation of nuclear magnetic shieldings for heavy nuclei has attracted great interest since its initial description,[54−57] and a few representative references of its discussion are given here.[54−63]

Specifically for the organophosphine selenides, because of the presence of ^{31}P (100% natural abundance), it is prudent to discuss the theory of spin−spin coupling. The concept of direct dipolar and indirect spin−spin coupling is well covered in the literature.[64−69] The direct dipolar, **D**, tensor is of second-rank and is traceless, while the indirect spin−spin, **J**, tensor is a general second-rank tensor with a nonzero trace. The average of the principal components of **J** (J_{11}, J_{22}, J_{33}) provides the isotropic indirect spin−spin coupling constant, J_{iso}. For directly bonded selenium-77 and phosphorus-31 spin pairs, $^1J(^{77}\text{Se},^{31}\text{P})$ values are known to be negative.[65,70] The anisotropy of the **J**-tensor is defined as $\Delta J = J_{33} - (J_{11} + J_{22})/2$ and is inherently linked with the direct dipolar coupling constant, R_{DD}; R_{DD} and ΔJ cannot be separated and an effective direct dipolar coupling constant, R_{eff}, is obtained experimentally:

$$R_{eff} = R_{DD} - \Delta J/3 \quad (2)$$

and

$$R_{DD} = \left(\frac{\mu_0}{4\pi}\right)\left(\frac{\hbar}{2\pi}\right)\left(\frac{\gamma_I\gamma_S}{\langle r_{IS}^3\rangle}\right) \quad (3)$$

where μ_0 is the permeability of a vacuum, γ_I and γ_S are the magnetogyric ratios of the coupled spins, I and S, and $\langle r_{IS}^3\rangle$ is the motionally averaged cube of the distance between the coupled nuclei. When the value of R_{eff} can be determined from an experimental spectrum, ΔJ can be estimated from eq 2 provided r_{IS} is known (eq 3). Previously, we have shown that the dipolar-splitting-ratio method can provide information on the orientation of the internuclear vector with respect to the chemical shift tensor principal components in powder samples containing an isolated spin pair.[71]

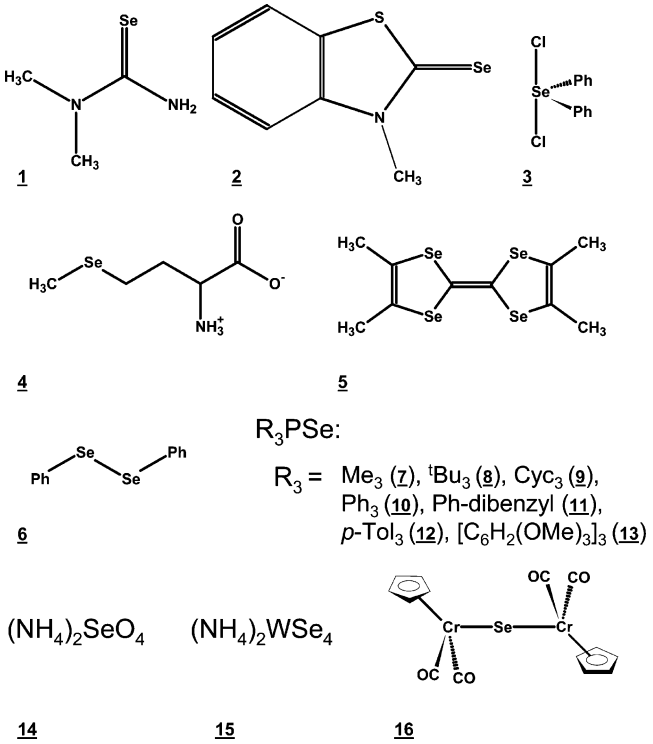

Figure 1. Compounds **1**−**16** investigated in this study.

Experimental Section

Representations of compounds **1**−**16** investigated in this study are given in Figure 1. The following samples were acquired from commercial sources and were used without further purification: *N*,*N*-dimethylselenourea (**1**) and diphenylselenium dichloride (**3**) from Strem; *N*-methylbenzothiazole-2-selone (**2**), tetramethyltetraselenafulvalene (**5**), and diphenyl diselenide (**6**) from Aldrich; seleno-DL-methionine (**4**) from Sigma; and ammonium selenate (**14**) and ammonium selenotungstate (**15**) from Alfa. The organophosphine selenides (**7**−**13**) were prepared from the appropriate phosphine and KSeCN, according to the procedure outlined in the literature.[72]

Selenium-77 NMR spectra were obtained at 38.154 and 76.277 MHz on Bruker MSL-200 and AMX-400 NMR spectrometers ($\mathbf{B}_0 = 4.7$ and 9.4 T), respectively. The samples were packed into 7 mm o.d. zirconium oxide rotors and were spun at magic-angle spinning (MAS) frequencies (ν_{rot}) between 1.5 and 6.2 kHz. Standard cross polarization (CP), or ramped-amplitude CP (RACP), and high-power ^{1}H decoupling were employed in acquiring all NMR spectra, except for cases where CP was so inefficient that improved results were obtained after a single pulse with ^{1}H decoupling and long recycle delays. Selenium chemical shifts were referenced to a neat liquid of dimethyl selenide (Me_2Se) at 23 °C by setting the isotropic NMR peak of solid $(NH_4)_2SeO_4$ to +1040.2 ppm.[73,74] Isotropic chemical shifts were identified by varying the spinning frequency. The principal components of the chemical shift tensors, δ_{ii}, were determined via the method of Herzfeld and Berger[75] except those for $(NH_4)_2SeO_4$, which were determined from the discontinuities in the spectrum of a stationary sample, and all spectra were simulated using the determined values with the program WSOLIDS[76] to assess the quality of the obtained parameters. This procedure results in errors of ±0.2 ppm in

the isotropic chemical shifts and errors in the principal components about 1−3% of the span of the respective chemical shift tensor.

Quantum chemistry calculations of magnetic shielding tensors were carried out using the NMR module[77−79] of the Amsterdam Density Functional (ADF) program package.[80−84] The Vosko−Wilk−Nusair[85] local density approximation with the Becke88−Perdew86[86−88] generalized gradient approximation was used for the exchange-correlation functional. Nonrelativistic (NR), scalar relativistic (SC), and scalar with spin−orbit relativistic (SO) calculations were performed to gauge the importance of relativistic effects for the calculation of NMR parameters involving selenium. The relativistic corrections carried out are based on the implementation of the ZORA formalism.[42−45] Triple-ζ doubly polarized, TZ2P, Slater-type ZORA basis sets were used for all atoms except for hydrogen, which received double-ζ quality, DZ, basis functions. The calculations were performed on a Linux-based cluster with either dual AMD MP 1800+ Athlon processor nodes or two AMD XP 1800+ Athlon processors operating in parallel.

The crystal structures for compounds **1**−**16** have previously been determined by X-ray diffraction (XRD).[89−104] The atomic coordinates for compound **12** could not be generated from the report in the literature[100] and were determined from a nonrelativistic geometry optimization using ADF basis sets of similar quality to those used in the magnetic shielding tensor calculations. All DFT calculations were carried out on isolated molecules using the non-hydrogen atomic coordinates, determined from the crystal structures where possible. For the ionic compounds **14** and **15**, NH_4^+ cations within 5.0 Å of the central atom in the anionic tetrahedron, SeO_4^{2-} or WSe_4^{2-}, were included in the calculations. Hydrogen atoms were placed at idealized positions (r_{CH} = 1.09 Å (alkyl) or 1.08 Å (aryl), r_{NH} = 1.02 Å). Herein, we use the labels "a", "b", and so forth to designate the difference between multiple sites, and a calculated value was assigned to the site that minimized the difference between the calculated and experimental values. The molecules were translated so that the selenium atoms were located at the origin to minimize a gauge variance for the calculation of the off-diagonal components of the magnetic shielding tensors within ADF 2004.01 and earlier versions.[80] Since the calculations were performed on isolated molecules, intermolecular interactions were not included. Solvent effects are known to affect the chemical shift for selenium compounds[18,22,105,106] and have been observed to vary by up to 50 ppm in organoselenium species.[22,107] Changes of phase are also known to influence selenium magnetic shielding tensors; for example, $\sigma_{iso}(^{77}Se)$ for H_2Se decreases by 126.6 ± 0.5 ppm when gaseous hydrogen selenide (5 atm) undergoes liquefaction and decreases further by 11.4 ± 0.2 ppm when liquid H_2Se freezes.[108] These potential effects must be considered when comparing calculated values to experimental solution and solid-state parameters.

The chemical shift tensors were determined from the calculated magnetic shielding tensors, and the value of $\sigma_{iso}(Me_2Se)$, calculated at the same level of theory, according to eq 1. Because of the lack of an experimentally determined structure, the geometry of Me_2Se was optimized and converged with a staggered−staggered orientation of the molecule consistent with previous investigations.[28,30−32] The calculated NR, SC, and SO values used for the isotropic shielding of dimethyl selenide were 1627.8, 1580.0, and 1745.2 ppm, respectively. These values are in agreement with those previously reported by other authors.[28,30−33,35,38,41,109−112]

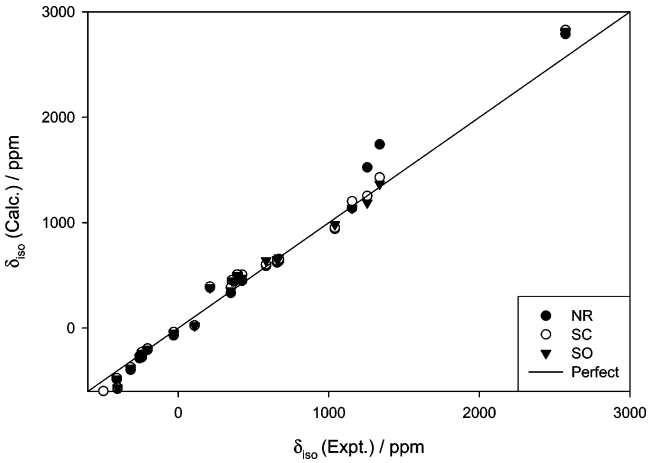

Figure 2. Experimental vs calculated isotropic chemical shifts, δ_{iso}, for the selenium-containing compounds investigated, **1**−**16**; the solid diagonal line indicates perfect agreement between calculated and experimental results.

Results and Discussion

Comparison of Observed and Calculated Selenium Chemical Shift Tensors. Experimental and computational results obtained in this investigation are summarized in Tables 1−3. The successes of the DFT computations in reproducing the experimental results obtained are illustrated in Figures 2−4. A plot of calculated versus experimental isotropic chemical shifts for all of the compounds investigated is given in Figure 2. All theoretical methods employed perform very well in reproducing δ_{iso} as evidenced by the small deviation of the individual points from the solid line that represents perfect agreement between experiment and theory. The agreement was expected as numerous approaches have been successful in reproducing isotropic selenium chemical shifts.[25,28,30−33,35,37−41,110] The largest discrepancy observed appears for the values of δ_{iso}(NR) calculated for two of the isotropic chemical shifts for ammonium selenotungstate, **15a** and **15b**.

Plots of theoretical versus experimental values for the individual principal components, δ_{ii}, of the selenium chemical shift tensors investigated are given in Figure 3. From Figure 3a, it is clear that the calculated values for δ_{11} reproduce the trend observed in the values of δ_{11} (expt.). The deviations of the individual points from the idealized line of perfect agreement are noticeably larger in magnitude than those found for the comparison of isotropic values. The plot emphasizes that the majority of the calculations tends to underestimate the magnitude of the shielding for this component, which leads to an overestimation of the value of δ_{11} (calc.) with respect to the corresponding experimental value; however, the inclusion of relativistic effects leads to better results in general.

Figure 3b displays a plot of calculated versus experimental values of δ_{22}. The trend observed in all of the experimentally determined intermediate principal components is well reproduced by δ_{22} (calc.). Unlike the δ_{11} component, there exists more balance in the instances of over- and underestimation of the calculated shielding in δ_{22} throughout the chemical shift tensors investigated, and relativistic effects do not appear to improve the agreement with experiment. The differences in magnitude between the individual points and the line of perfect agreement are generally larger than those observed for δ_{iso} (calc.) in Figure 2.

When the experimental and calculated values of δ_{33} are plotted against each other (Figure 3c), there are a couple points worth noting. First, the largest single deviation of any δ_{ii} (calc.)

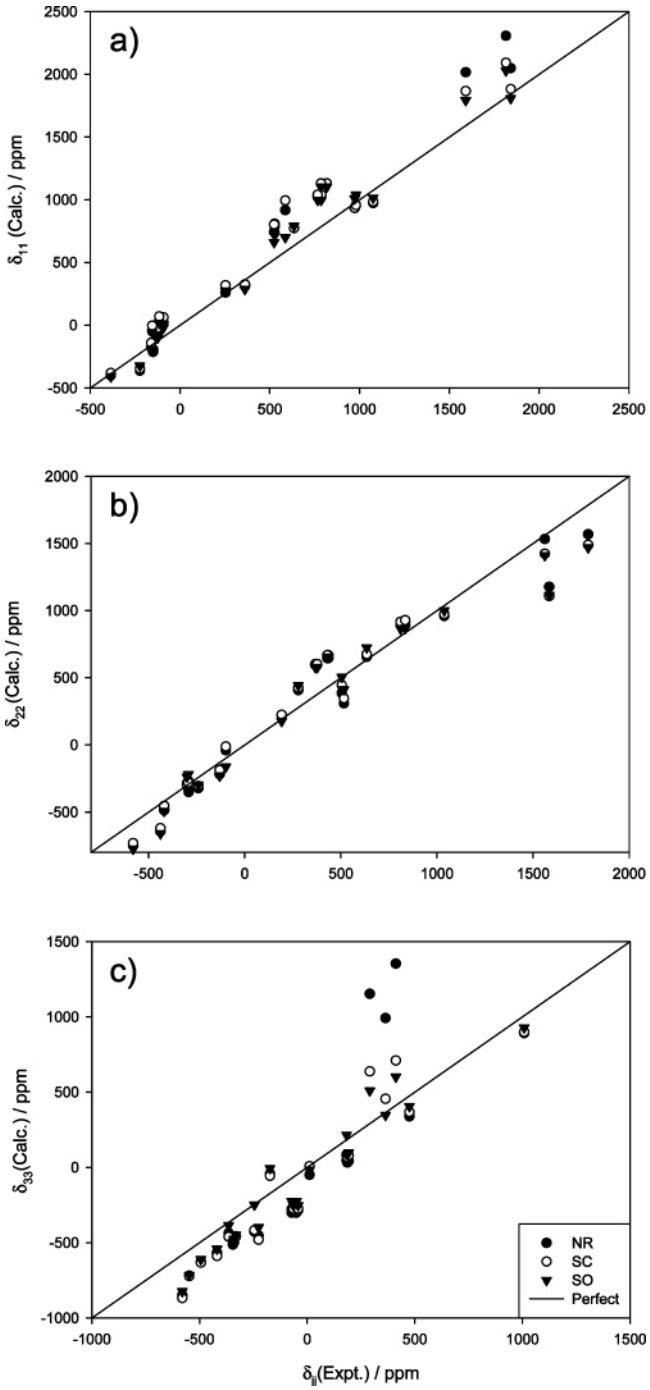

Figure 3. Experimental vs calculated values for (a) δ_{11}, (b) δ_{22}, and (c) δ_{33} for the selenium-containing compounds investigated, **1**−**15**; the solid diagonal line indicates perfect agreement between calculated and experimental results.

from its corresponding experimental value is observed in the calculation of δ_{33} for one of the three sites of $(NH_4)_2WSe_4$, **15a**. The values of δ_{33}(NR) for each of the three crystallographically nonequivalent selenium environments of ammonium selenotungstate, **15**, display substantially large deviations from their corresponding experimentally determined principal component. Second, aside from the δ_{33} (calc.) values for $(NH_4)_2WSe_4$ and a few other exceptions, the majority of the δ_{33} components are calculated to be more shielded, resulting in smaller values of δ_{33}, than is found experimentally.

Magnifying the accuracy of the calculations for the most and least shielded principal components, the experimentally determined spans of all of the compounds investigated are compared

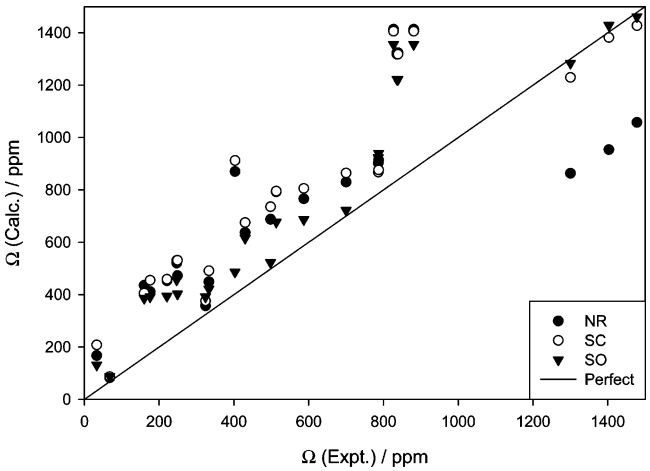

Figure 4. Experimental vs calculated spans, $\Omega = \delta_{11} - \delta_{33}$, for the selenium-containing compounds investigated, **1**−**15**; the solid diagonal line indicates perfect agreement between calculated and experimental results.

with their theoretical counterparts in Figure 4. For the most part, the spans are overestimated except for the nonrelativistic calculation of the three chemical shift tensors of $(NH_4)_2WSe_4$. This observation was expected given the generally observed overestimation of δ_{11} and underestimation of δ_{33} by the calculations (Figure 3). On the other hand, these errors cancel each other in their combined effect on δ_{iso}, leading to apparent agreement between theoretical and calculated values (Figure 2).

The results presented, and illustrated in Figures 2−4, indicate that the overall agreement between all of the DFT calculations and experiment is good, given the fact that the computations are performed on isolated molecules and that the experiments are performed on solid materials. In the following subsections, we shall focus, highlighting the exceptions to the general trends observed for the calculations, on the three classes of compounds investigated: (1) organoselenium compounds **1**−**6**, (2) organophosphine selenides **7**−**13**, and (3) inorganic selenium compounds **14**−**16**.

(1) Organoselenium Compounds. The range of molecular environments that selenium can be found in for organoselenium compounds is vast. The diversity of selenium environments in the representative compounds investigated provides a good test of the theoretical methods employed.

1. *N*,*N*-Dimethylselenourea is a relatively simple selenocarbonyl, or selone, compound for solid-state NMR investigation. The experimental and simulated spectra for **1** are given in Figure 5. The experimental spectrum was simulated using the parameters obtained from a Herzfeld−Berger analysis and given in Table 1. The chemical shift tensor for selenium in this compound has not previously been reported; however, some solution ^{77}Se NMR has been performed.[113] The isotropic chemical shift obtained for the solid, 211 ppm, is somewhat deshielded relative to the solution value of 147 ppm,[113] both of which are common values obtained for selenocarbonyls possessing nitrogen substituents. The difference between the two shifts is not surprising given the effect of intermolecular interactions.[18]

The calculated isotropic selenium chemical shifts for **1** using the NR, SC, and SO methods are in reasonable agreement with each other (Table 1); however, all three methods overestimate the experimental value of 211 ppm. Unlike the majority of the compounds investigated herein, the value of δ_{33} (calc.) is not underestimated by the calculations but is one of the few that slightly overestimates this component. The span of the chemical

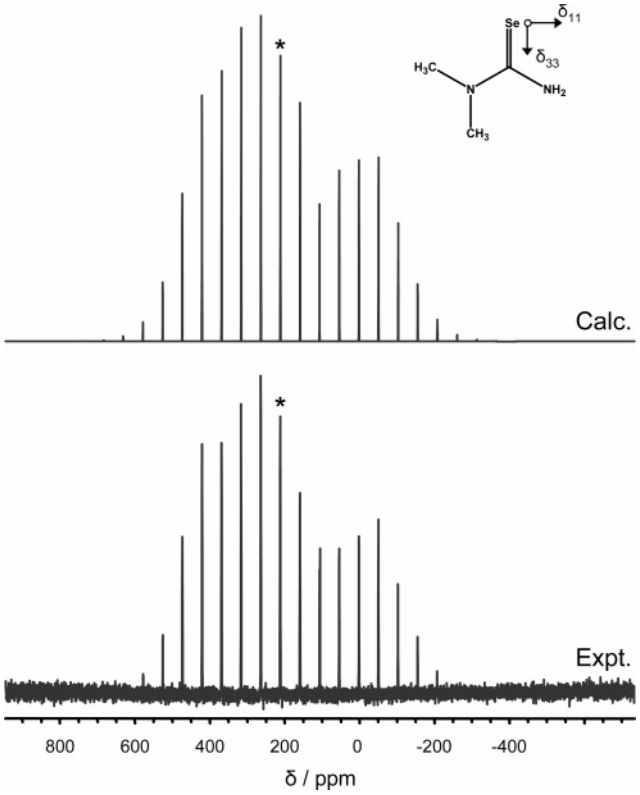

Figure 5. Simulated and experimental CPMAS ^{77}Se NMR spectra of *N*,*N*-dimethylselenourea (**1**), acquired at 9.4 T, after 48 transients, spinning at 4.0 kHz, with 50 Hz of line broadening, a contact time of 10.0 ms, and a 30 s pulse delay. The isotropic peak is labeled with an asterisk (*). Inset is a schematic of compound **1** showing the orientation of the selenium chemical shift tensor calculated at the scalar with spin−orbit relativistic level of theory.

shift tensor is overestimated at both the nonrelativistic and scalar relativistic levels of theory; however, the spin−orbit relativistic calculation accurately reproduces the experimental value of Ω. Thus, the value of δ_{33} (calc.) does not balance the corresponding overestimated value of δ_{11} (calc.) to obtain a calculated isotropic chemical shift that is in good agreement with the experimental value of **1**, as with the majority of the compounds investigated.

The orientations of the principal components calculated at all levels of theory are consistent in determining that the direction of greatest shielding, δ_{33}, lies approximately along the C−Se vector, the intermediate principal component, δ_{22}, is directed nearly perpendicular to the N−C−Se plane, and δ_{11}, orthogonal to the others, is slightly removed from coinciding with the N−C−Se plane (inset Figure 5). For comparison purposes, the orientation of the ^{17}O chemical shift tensor in urea has δ_{11} within the N−C−O plane, perpendicular to the C−O vector which is similar to the selenium homologue; however, it is the δ_{22} and not the δ_{33} component that is oriented parallel to the chalcogen−carbon vector in urea.[114] The difference between the two orientations is likely a result of a larger paramagnetic (deshielding) effect in the N−C−Se plane of **1** than in the N−C−O plane of urea. This results in a larger principal component directed perpendicular to the respective plane than parallel to the carbon−chalcogen vector in the selenium species.

2. *N*-Methylbenzothiazole-2-selone is a nearly planar molecule containing an aromatic ring with a selenocarbonyl functional group (see Figure 1). This appears to be the first reported ^{77}Se NMR investigation of this compound. The ^{77}Se NMR spectrum of **2**, Figure 6, acquired with MAS clearly shows four isotropic peaks, and four unique ^{77}Se chemical shift tensors are recorded for the as-received sample in Table 1. The crystal structure for *N*-methylbenzothiazole-2-selone suggests that only two nonequivalent selenium atoms are present in the unit cell.[90] The XRD identification was performed on only one of the two crystalline forms obtained from a methylene chloride recrystallization of the sample, stating that the other form was not suitable for X-ray investigation.[90] The isotropic chemical shifts for all four of the tensors obtained for this sample are very

TABLE 1: Experimental and Theoretical Chemical Shift Tensors[a] for Organoselenium Compounds

	δ_{iso}	δ_{11}	δ_{22}	δ_{33}	Ω
1					
expt.[b]	211	527	279	−173	700
expt.[c]	147				
NR	384	787	407	−42	829
SC	392	808	425	−56	864
SO	383	715	442	−7	722
2a					
expt.[b]	368	786	368	−50	836
	357	767	377	−72	839
NR	438	1022	594	−301	1323
SC	455	1040	602	−278	1318
SO	449	997	576	−225	1222
2b					
expt.[b]	396	817	435	−64	881
	392	785	430	−42	827
NR	496	1128	645	−285	1413
SC	508	1131	668	−274	1405
SO	501	1102	655	−253	1355
3					
expt.[b]	584	635	635	475	160
expt.[d]	574.9				
NR	588	773	654	338	435
SC	605	773	675	368	405
SO	640	791	723	405	386
4					
expt.[b]	109	361	192	−226	587
expt.[e]	112	369	202	−236	605
NR	26	312	221	−454	766
SC	23	325	224	−480	805
SO	21	287	176	−399	686
5a					
expt.[b]	657	973	811	187	786
expt.[f]	657.5	969.5	817.5	185.5	784
NR	621	934	898	32	902
SC	639	934	916	66	868
SO	653	1009	864	86	923
5b					
expt.[b]	669	980	835	193	787
expt.[f]	669.7	981.7	829.7	197.7	784
NR	636	956	909	42	914
SC	655	956	928	80	876
SO	668	1038	867	99	939
6a					
expt.[b]	350	524	516	11	513
expt.[g]	350	537	510	2	535
NR	333	742	308	−50	792
SC	385	803	345	8	795
SO	352	661	412	−16	677
6b					
expt.[b]	425	586	505	183	403
expt.[g]	425	565	527	183	382
NR	449	916	385	46	870
SC	507	994	444	83	911
SO	474	701	505	215	486

[a] Chemical shifts in ppm with respect to external Me_2Se. [b] This work. [c] Reference 113. [d] Reference 130. [e] Reference 131. [f] Reference 73. [g] Reference 111.

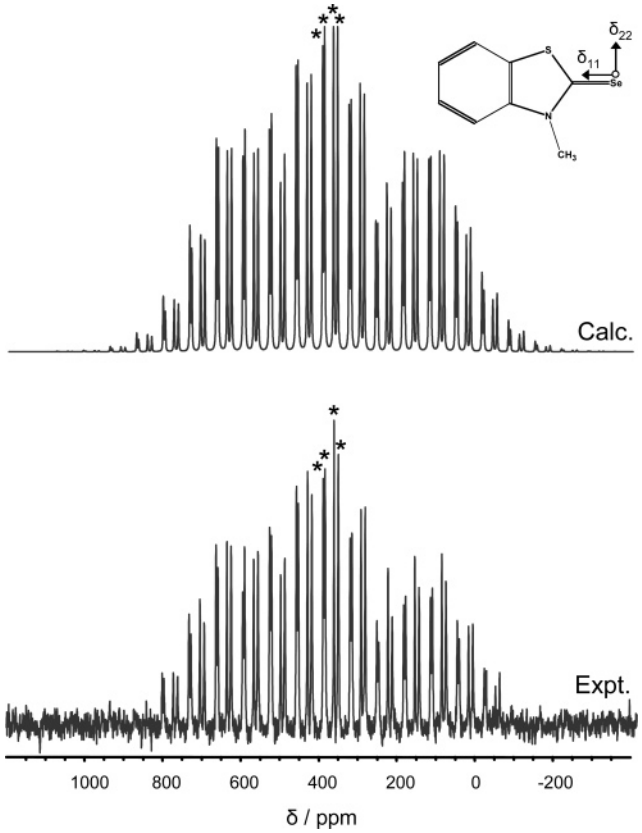

Figure 6. RACPMAS ^{77}Se NMR spectrum and the simulated spectrum of *N*-methylbenzothiazole-2-selone (**2**). Experimental parameters: 9.4 T, 1868 scans, 5.2 kHz MAS, with line broadening of 50 Hz applied, a 10.0 ms contact time, and a 20 s recycle delay. The isotropic peaks are labeled with an asterisk (*). Inset is a schematic of compound **2** showing the orientation of the selenium chemical shift tensor calculated at the scalar with spin−orbit relativistic level of theory.

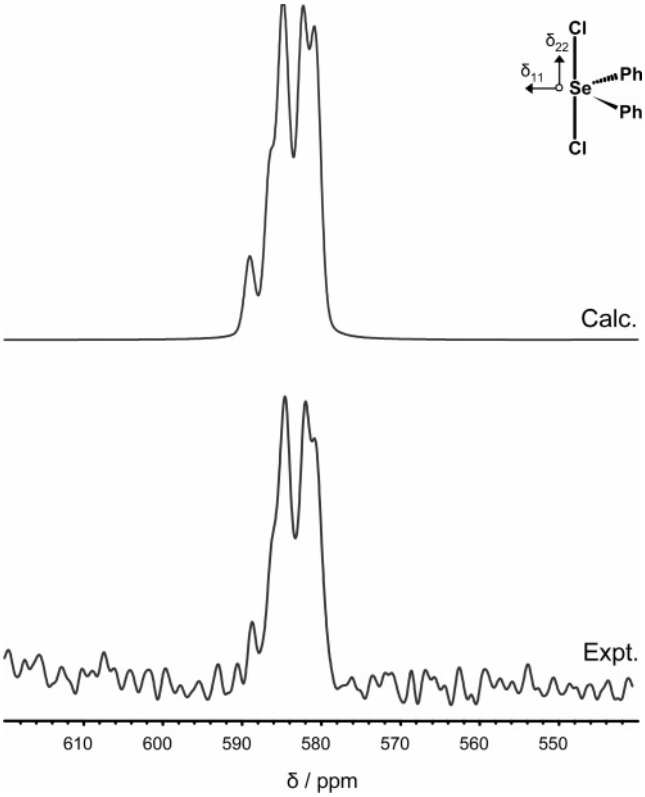

Figure 7. Selenium-77 RACPMAS NMR center band (spinning sidebands summed in) spectrum of compound **3**: Ph_2SeCl_2 (9.4 T, 972 scans, ν_{rot} = 4.0 kHz, 50 Hz line broadening, 10.0 ms contact time, 60 s pulse delay), and its simulation. Inset is a schematic of compound **3** showing the orientation of the selenium chemical shift tensor calculated at the scalar with spin−orbit relativistic level of theory.

similar and are in agreement with related compounds containing the C═Se moiety in which the carbon is bonded to one or more nitrogen atoms.[18] A study of ^{77}Se T_1 relaxation mechanisms of several selones in solution indicated chemical shift anisotropies of about 3000−6000 ppm,[115] which appear overestimated given the data for **1** and **2**. However, the same study reported a chemical shift anisotropy of 400 ppm for **6**, which is in line with our findings (vide infra).

There are a pair of chemical shift tensors, however, that might be distinguishable from the other via calculation of their respective magnetic shielding tensors, and these pairs have been identified as **2a** and **2b** corresponding to the tensors with the two smallest and the two largest isotropic chemical shifts, respectively. Each of the two selenium magnetic shielding tensors calculated from the crystal structure of **2** is compared with the pair of experimental selenium chemical shift tensors that each corresponds most closely with. While this assignment is arbitrary, it is noted that for all calculations the site with the smaller isotropic ^{77}Se chemical shift also has a smaller span, and the larger δ_{iso} (calc.) was obtained from the trace of a tensor with a broader extent of shielding. The attributes of these calculated chemical shift tensors are mimicked in the distinctions between the pairs of experimental tensors labeled **2a** and **2b**. The differences between the calculated isotropic values of sites **2a** and **2b** at all levels of theory are similar to those between the pairs of experimental tensors. The general trends observed for the majority of the calculations in Figures 2−4 hold for both calculated chemical shift tensors in **2**. Identical orientations for the calculated shielding tensors are obtained, regardless of the level of theory employed. The direction of δ_{11} lies nearly coincident with the C−Se vector, and δ_{33} is perpendicular to the molecular plane, as illustrated inset within Figure 6. The orientations obtained for **2** are different from both the orientations obtained for ^{77}Se in **1** and for ^{17}O in urea;[114] however, the calculated ^{77}Se chemical shift tensors for **2** are oriented nearly identically to the ^{17}O chemical shift tensor determined for benzamide.[116] The similarities and differences between the orientations of ^{17}O and ^{77}Se chemical shift tensors in ketones and selones suggest that the shielding interaction in selenocarbonyl compounds is at least as complicated as their oxygen counterparts and is very sensitive to the environment of this functional group.

3. Diphenylselenium dichloride provides a four-coordinate environment around the selenium in which the molecule adopts a seesaw configuration with a Cl−Se−Cl angle of approximately 180(5)°.[91] The calculated and experimental isotropic ^{77}Se NMR spectra for **3** are given in Figure 7. The selenium nucleus experiences residual dipolar coupling[117−125] from the quadrupolar chlorine nuclei ($^{35/37}$Cl), with a residual dipolar coupling constant of 41 Hz at 9.4 T. On the basis of the ^{35}Cl NQR frequency of 23.076 MHz provided by an NQR study for **3**,[126,127] and the Se−Cl distance of 2.30 Å,[91] a residual dipolar coupling constant of 65 Hz was anticipated. An indirect spin−spin coupling constant, ^1J (^{77}Se,^{35}Cl)$_{iso}$, of 110 Hz is observed and appears to be the first reported coupling between selenium and chlorine. Indirect spin−spin coupling has previously been reported between tellurium-125 and chlorine-35 in $Me_3TeCl{\cdot}H_2O$,[128] in which the ^{125}Te is coupled to two ^{35}Cl nuclei similar to the environment observed in **3**. Scaling of ^1J (^{125}Te,^{35}Cl)$_{iso}$ by $4\pi^2/h\gamma_{Te}\gamma_{Cl}$ to yield the reduced coupling

constant, ^1K (Te,Cl), 283×10^{19} T^2 J^{-1} indicates that the corresponding value of 487×10^{19} T^2 J^{-1} for ^1K (Se,Cl) in **3** is of an appropriate magnitude. The principal components, δ_{ii} (Table 1), determined in the simulation indicate an axially symmetric chemical shift tensor. There are, however, no symmetry reasons for the chemical shift tensor to attain this axial symmetry. It is known that methods for obtaining the principal components of the chemical shift tensor from spectra of MAS samples have the greatest difficulty with axially or near axially symmetric species.[129] The isotropic chemical shift, $\delta_{iso} = 584$ ppm, agrees well with the value obtained for **3** in a chloroform solution, $\delta_{iso} = 575$ ppm.[130]

All of the calculated principal components of the ^{77}Se chemical shift tensor, given in Table 1, fail to reproduce the observed axial symmetry and the small span obtained for Ph_2SeCl_2 experimentally. The orientations determined from each of the calculations were in agreement with each other. The direction of δ_{11} is predicted to bisect the $C_{ipso}-Se-C'_{ipso}$ angle, that is, corresponds to the direction of the formal "lone pair". The intermediate principal component, δ_{22}, is parallel to the approximately linear Cl−Se−Cl vector, and δ_{33} perpendicular to the other two components lies in the $C_{ipso}-Se-C'_{ipso}$ plane (inset Figure 7).

4. Seleno-DL-methionine is a seleno-amino acid in which the sulfur in methionine has been replaced with selenium (Figure 1). A solid-state ^{77}Se NMR investigation of this compound has been reported by Potrzebowski et al.,[131] and our parameters agree very well with those obtained in their investigation (Table 1). For selenium in a similar dialkyl environment, a selenium coronand, Batchelor et al. reported isotropic chemical shifts from 173 to 737 ppm for the four crystallographically nonequivalent selenium atoms, with spans ranging from less than 370 to 771 ppm.[132]

The NR, SC, and SO calculations of the chemical shift tensor principal components for seleno-DL-methionine are in very good agreement with the experimental results (Table 1). Deviating from the general trend observed for the calculations in Figure 3a, the shielding along the δ_{11} direction is in reasonable agreement with the experimental value, if not slightly overestimated. The magnetic shielding tensor's calculated orientation, by all methods, is such that δ_{11} lies approximately along the $Se-C_{terminal}$ bond axis, δ_{22} is directed perpendicular to the $C_\gamma-Se-C_{terminal}$ plane, and the smallest principal component of the chemical shift tensor, δ_{33}, is nearly parallel to the bond axis between the γ-carbon and selenium. Potrzebowski et al. did not perform any theoretical calculation of the selenium chemical shift tensor in **4**;[131] however, the orientation that they assumed is in accord with those determined by our DFT calculations.

5. Similar to the sulfur analogues,[133] tetraselenafulvalenes are precursors for conducting and superconducting materials.[93] The crystal structure of **5** contains an inversion center within the molecule such that only two of the selenium atoms within the molecule are expected to give rise to unique chemical shift tensors.[93] The values obtained for the two sets of principal components observed are in very good agreement with a previous solid-state ^{77}Se NMR investigation of this compound by Collins et al. (Table 1).[73] The chemical shift tensors are nearly identical indicating that the electronic environments of the magnetically nonequivalent selenium atoms are very similar. Comparable isotropic chemical shifts, 408−624 ppm, and spans, 554−687 ppm, have been reported for a series of 1,3-selenazoles which possess selenium in a similar environment to the tetraselenafulvalenes.[134]

All theoretical methods perform equally well in reproducing the experimentally determined principal components for **5a** and **5b** (Table 1). The calculated orientations of the chemical shift tensors are predicted to be the same for both **5a** and **5b** and are consistent across all of the methods employed. The direction of δ_{11} is predicted to bisect the C−Se−C angle, δ_{22} is oriented perpendicular to the molecular plane, and δ_{33} is calculated to be within the skeletal molecular plane, directed close to the Se−C vector of the Se−C−Se component of the molecule.

6. Diselenides, the selenium equivalent of organic peroxides, are an intriguing functional group as they possess glutathione

TABLE 2: Experimental and Theoretical Chemical Shift Tensors[a] for Tris-organophosphine Selenides

	δ_{iso}	δ_{11}	δ_{22}	δ_{33}	Ω
7					
expt.[b]	−204	−116	−130	−365	249
expt.[c]	−199.6	−117.7	−131.7	−349.3	231.6
NR	−207	35	−219	−437	472
SC	−193	70	−188	−461	531
SO	−200	17	−231	−385	402
8					
expt.[b]	−408	−386	−419	−419	33
expt.[d]	−414.5				
NR	−485	−401	−486	−568	167
SC	−475	−381	−455	−589	208
SO	−481	−410	−493	−541	131
9					
expt.[b]	−437	−150	−580	−580	430
expt.[e]	−466.4				
NR	−603	−213	−745	−850	637
SC	−598	−193	−732	−868	675
SO	−602	−208	−776	−823	615
10a					
expt.[b]	−257	−124	−300	−345	221
expt.[c]	−257.5	−122.5	−288.4	−361.5	239.0
NR	−286	−59	−288	−512	453
SC	−267	−20	−303	−478	458
SO	−277	−100	−238	−494	394
10b					
expt.[b]	−242	−93	−293	−340	247
expt.[c]	−242.6	−86.2	−264.1	−377.4	291.2
NR	−249	22	−270	−498	520
SC	−228	63	−281	−467	530
SO	−239	−20	−220	−476	456
11a					
expt.[b]	−316	−161	−292	−494	333
expt.[f]	−364.7				
NR	−396	−178	−352	−627	449
SC	−370	−142	−336	−633	491
SO	−379	−191	−334	−611	420
11b					
expt.[b]	−403	−224	−438	−548	324
expt.[f]	−364.7				
NR	−576	−363	−646	−720	357
SC	−563	−347	−620	−723	376
SO	−567	−324	−661	−715	391
12					
expt.[b]	−242	−155	−241	−331	176
expt.[g]	−264				
NR	−277	−49	−322	−460	411
SC	−256	−4	−306	−458	454
SO	−267	−57	−297	−448	391
13					
expt.[b]	−30	253	−98	−245	498
expt.[g]	−28.4				
NR	−70	260	−42	−428	688
SC	−37	318	−12	−417	735
SO	−46	273	−163	−249	522

[a] Chemical shifts in ppm with respect to external Me_2Se. [b] This work. [c] Reference 27. [d] Reference 140. [e] Reference 141. [f] Reference 143. [g] Reference 145.

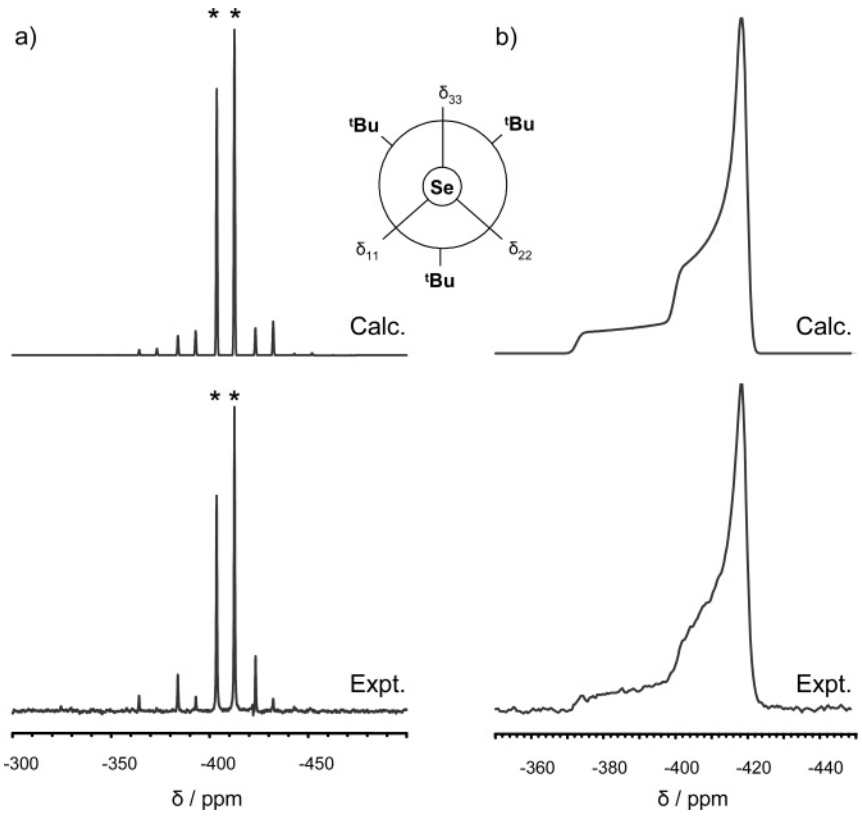

Figure 8. (a) CPMAS ^{77}Se NMR spectrum and its simulation of ^{t}Bu$_3$PSe (**8**) at 9.4 T, after 88 scans, 1.5 kHz MAS, 30 Hz of line broadening, a contact time of 4.0 ms, and a recycle delay of 4 s. The *J*-coupled isotropic peaks are labeled with asterisks (*). (b) Experimental and simulated CP ^{77}Se NMR spectra of stationary **8**. Experimental conditions: 9.4 T, 6116 transients, 200 Hz line broadening, a 4.0 ms contact time, and a 10 s pulse delay. Inset is a Newman projection along the P−Se bond of compound **8** showing the orientation of the selenium chemical shift tensor calculated at the scalar with spin−orbit relativistic level of theory.

peroxidase-like activity.[135−139] The Bloch decay spectrum (not shown) indicates two selenium environments with distinct chemical shift tensors. The number of sites and their parameters agree well with a previous solid-state ^{77}Se CPMAS investigation of compound **6**,[111] specifically in the large difference in the most shielded component, δ_{33}, of the two tensors **6a** and **6b** (Table 1).

The spin−orbit calculation produces a more accurate value of the span for **6b** because of an increased accuracy in the values for both δ_{11} and δ_{33}. The more accurate values of δ_{ii} (calc.) from the SO calculation indicate a contribution from spin−orbit coupling, likely in part from the presence of the directly bonded selenium. The calculated orientations for the two selenium shielding tensors in diphenyl diselenide are nearly identical. The direction of greatest shielding, δ_{33}, most closely approaches a parallel direction to the Se−Se bond vector, δ_{22} bisects the Se−Se−C_{ipso} angle, and the largest principal component of the chemical shift tensor, δ_{11}, is oriented perpendicular to the Se−Se−C_{ipso} plane. Theoretical studies[111] indicated that the differences in the chemical shift anisotropy mainly result from a β-effect of the torsional angle for the phenyl group at the next selenium, not the directly bonded phenyl group.

The chemical shift tensors investigated for compounds **1**−**6** are shown to represent the chemical diversity of these organoselenium species and are calculated similarly with and without the consideration of relativistic effects.

(2) Organophosphine Selenides. The organophosphine selenides, R_3PSe, provide an opportunity to investigate many peripheral modifications to one specific functional group.

7. The selenium chemical shift tensor principal components of Me_3PSe, from Herzfeld−Berger analysis of the MAS spectrum (not shown), and indirect spin−spin coupling parameters, J_{iso} and ΔJ, are in good agreement with those of an investigation by Grossmann et al. on 70% ^{77}Se enriched **7** (see Table 2).[27] There exists a single selenium environment that is coupled to the phosphorus with an indirect spin−spin coupling constant, ^1J (^{77}Se,^{31}P)$_{iso}$, of −656 Hz, and a direct dipolar coupling constant of 990 Hz (calculated from $r_{P-Se} = 2.111$ Å[95]), which results in a value of 700 Hz for ΔJ (eq 2).

The crystal structure for **7** does not possess a C_3 symmetry axis along the P−Se bond,[95] and thus three distinct principal components are calculated consistent with the nonaxially symmetric chemical shift tensor observed experimentally. The calculated chemical shift tensors at the NR, SC, and SO levels of theory are compared in Table 2 with the experimental values obtained herein and by Grossmann et al.[27] for solid Me_3PSe. The deviation in the calculations of the individual principal components manifests itself in larger spans. All of the calculations produce similarly oriented tensors, predicting that δ_{33} lies approximately along the P−Se vector. This is in agreement with the simulation of the ^{77}Se NMR spectrum of a stationary sample (not shown) and with a dipolar-splitting-ratio method investigation of this compound.[27]

8. Figure 8 shows the calculated and experimental spectra obtained for tris-(*tert*-butyl)phosphine selenide (^{t}Bu$_3$PSe) under MAS and stationary conditions. The MAS spectrum yields the components of the selenium chemical shift tensor as well as the isotropic spin−spin coupling constant, ^1J (^{77}Se,^{31}P)$_{iso}$, −693 Hz. The principal components of the chemical shift tensor given in Table 2 are the first to be reported for compound **8**. The solid-state values of δ_{iso} and ^1J (^{77}Se,^{31}P)$_{iso}$ agree well with the values obtained from ^{31}P and ^{77}Se solution NMR.[140] The

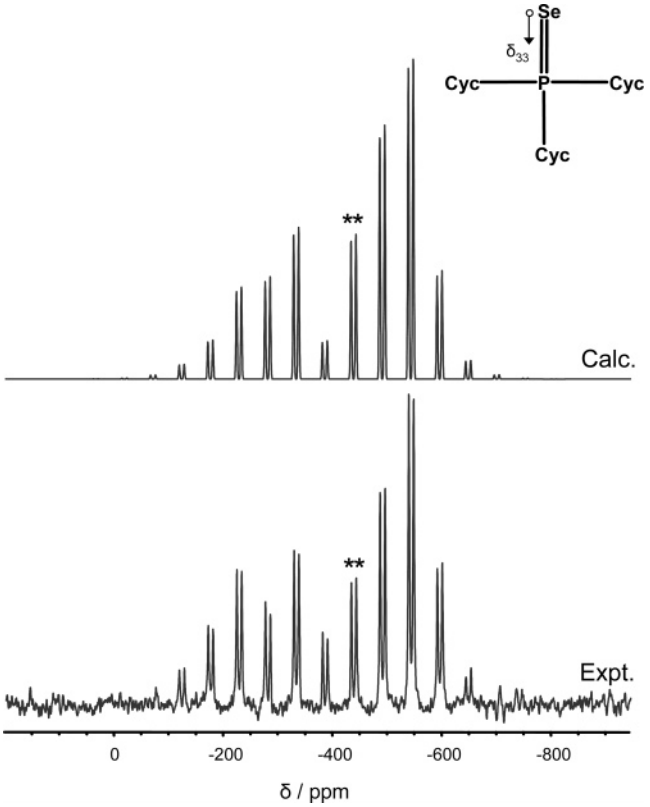

Figure 9. Selenium-77 RACPMAS NMR and calculated spectra for Cyc_3PSe (**9**). Experimental conditions: 9.4 T, 4912 scans, spinning at 4.0 kHz, 300 Hz of line broadening, a 1.0 ms contact time, and a 20 s recycle delay. The *J*-coupled isotropic peaks are labeled with asterisks (*). Inset is a schematic of compound **9** showing the orientation of the selenium chemical shift tensor calculated at the scalar with spin−orbit relativistic level of theory.

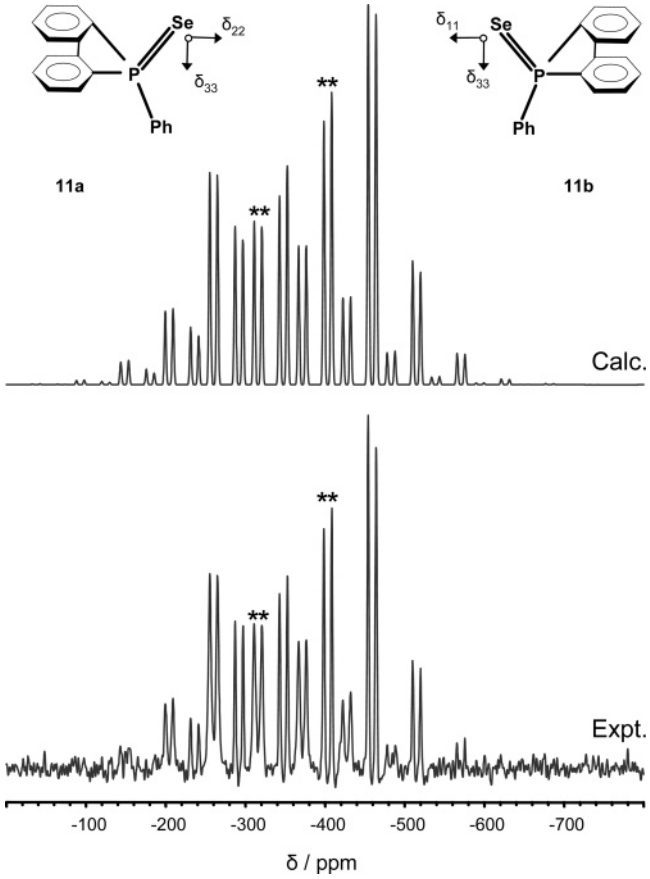

Figure 10. 5-Phenyldibenzophosphine 5-selenide (**11**) simulated and experimental RACPMAS ^{77}Se spectra obtained at 9.4 T, 2906 scans, 4.2 kHz MAS, line broadened by 80 Hz, a 15.0 ms contact time, and a pulse delay of 60 s. The *J*-coupled isotropic peaks are labeled with asterisks (*). Insets are schematics of compounds **11a** and **11b** showing the orientation of the selenium chemical shift tensors calculated at the scalar with spin−orbit relativistic level of theory.

spectrum of a stationary sample, together with the information obtained from the MAS spectrum, yields the effective dipolar coupling constant, R_{eff}, of 660 Hz. The dipolar coupling constant, R_{DD}, is calculated to be 960 Hz ($r_{PSe} = 2.133$ Å[96]) requiring a ΔJ of 900 Hz (eq 2).

The δ_{ii} values obtained from the ZORA DFT calculations for $^tBu_3PSe$ do not reproduce the experimental values or their orientations, which is not surprising considering the extremely small span observed, Ω (expt.), of 33 ppm. From the dipolar-splitting-ratio analysis of the spectrum of a stationary sample (Figure 8b) and the known molecular environment, the unique component of shielding, δ_{11}, should lie along the direction of the P−Se bond. The NR and SC calculations incorrectly predict that δ_{33} is closest to the P−Se vector, and the SO calculation determines that all of the principal components are approximately equidistant from the internuclear vector (inset Figure 8).

9. The calculated and experimental spectra of MAS samples for tricyclohexylphosphine selenide (Cyc_3PSe) are given in Figure 9. Because of the length of time required to obtain the MAS spectrum, the corresponding spectrum of a stationary sample for **9** was not acquired. The principal components of the chemical shift tensor are given in Table 2, and the isotropic chemical shift agrees well with the solution value previously reported.[141] A value of −682 Hz for $^1J(^{77}Se,^{31}P)_{iso}$ was obtained, which compares very well with the values obtained from a solution and solid-state ^{31}P NMR investigation.[97]

The majority of the observed trends for the calculations are upheld in the calculation of the chemical shift tensor for **9**. A specific exception occurs for δ_{11} (calc.) where the shielding is overestimated compared to the experimentally determined value. Despite this, the larger than experimentally observed values of Ω (calc.) are a result of the small calculated values of δ_{33}. All calculations predict that the δ_{33} component is closest to the P−Se vector, as shown inset in Figure 9.

10. There are two nonequivalent Ph_3PSe molecules in the unit cell.[98] The chemical shift tensors have been labeled in the same manner as in a previous investigation of **10** by Grossmann et al.,[27] and our values obtained at natural abundance agree well with those obtained from their investigation on 70% ^{77}Se enriched **10**. The isotropic spin−spin coupling constants obtained, −733 and −736 Hz for **10a** and **10b**, are also in agreement with values reported earlier.

The calculations for the two nonequivalent selenium environments, **10a** and **10b**, given in Table 2 show slight variation between the computational methods employed and adhere to the general trends shown in Figures 2−4. The calculated orientations for the chemical shift tensors for the selenium atoms in **10a** and **10b** are unique to the organophosphine selenides investigated in that it is δ_{22} that lies approximately along the P−Se direction, and this is consistent with the orientation obtained from a dipolar-splitting-ratio method investigation of 70% enriched $Ph_3P^{77}Se$.[27] The orientation shows some parallels with the ^{17}O chemical shift tensors in the monoclinic and orthorhombic forms of Ph_3PO, where both crystallographic forms have δ_{11} oriented along the P−O vector.[142] With δ_{11} along the P−O direction in Ph_3PO, it was inferred from the value of the shielding that the bonding environment is more appropriately

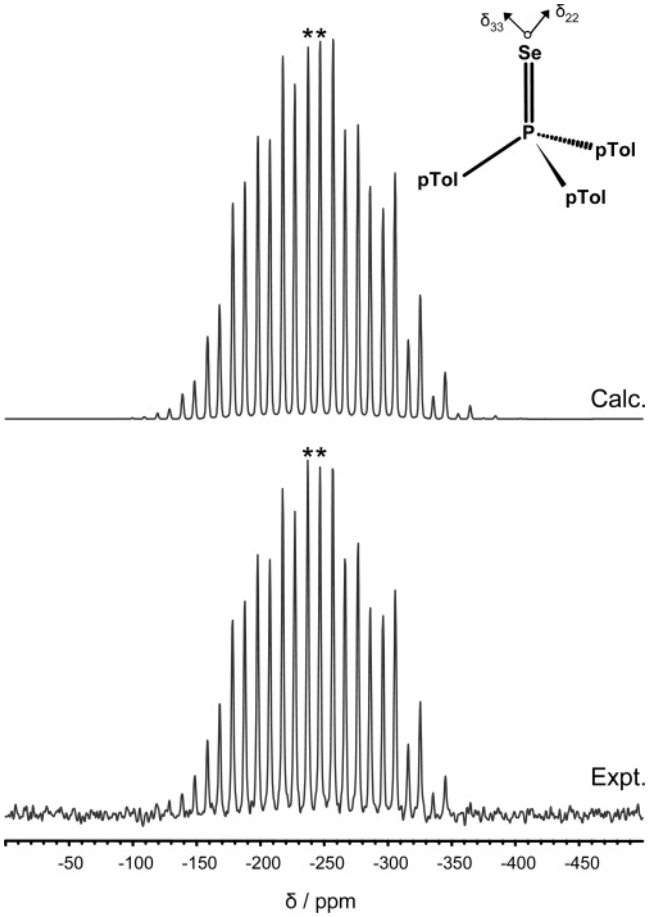

Figure 11. CPMAS ^{77}Se NMR spectrum and the calculated spectrum for *p*-Tol$_3$PSe (**12**). Experimental parameters: 9.4 T, 642 transients, 1.5 kHz MAS, 30 Hz line broadening, a contact time of 15.0 ms, and a 30 s recycle delay. The *J*-coupled isotropic peaks are labeled with asterisks (*). Inset is a schematic of compound **12** showing the orientation of the selenium chemical shift tensor calculated at the scalar with spin−orbit relativistic level of theory.

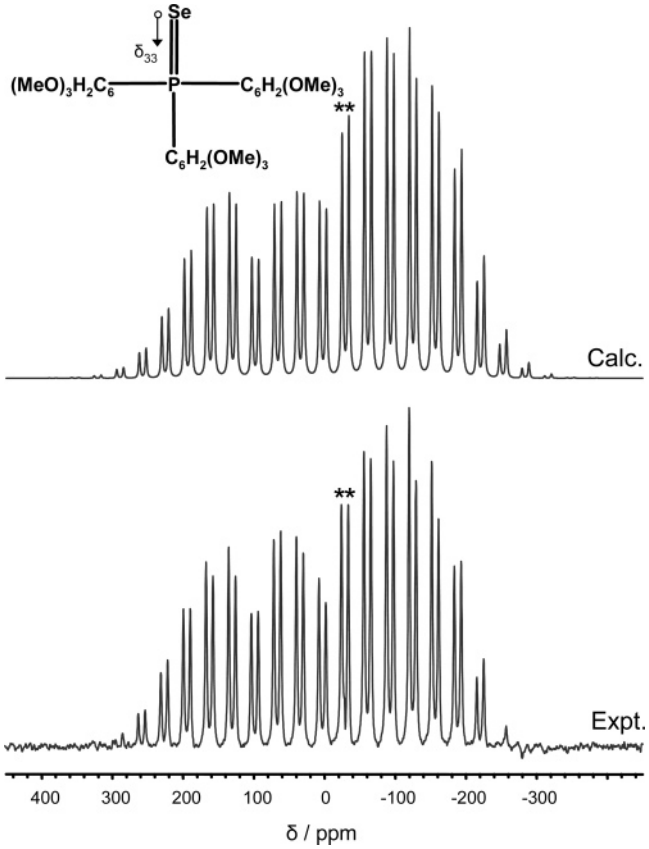

Figure 12. Experimental ^{77}Se CPMAS NMR and calculated spectra for TTMPSe (**13**) at 9.4 T. Experimental parameters: 15212 scans, spinning at 2.4 kHz, 100 Hz of line broadening, a 10.0 ms contact time, and a 4 s pulse delay. The *J*-coupled isotropic peaks are labeled with asterisks (*). Inset is a schematic of compound **13** showing the orientation of the selenium chemical shift tensor calculated at the scalar with spin−orbit relativistic level of theory.

represented by $Ph_3P^+-O^-$ according to Ramsey's theory of nuclear magnetic shielding.[51,52] In both chemical shift tensors for **10**, δ_{22} lies along the P−Se vector and indicates that a similarly small deshielding occurs along this direction consistent with a polarized, $Ph_3P^+-Se^-$, description of the phosphorus−selenium bond.

11. The spectrum of an MAS sample for 5-phenyldibenzophosphine 5-selenide and its best-fit simulation are given in Figure 10. While similar in skeletal structure and number of molecules in the asymmetric unit to **10**, **11** possesses a dibenzophosphole moiety (inset of Figure 10). A spectrum of a stationary sample could not be obtained in a reasonable amount of time to afford sufficient analysis. The isotropic chemical shifts, −316 and −403 ppm, and indirect spin−spin coupling constants, −733 and −768 Hz, for **11a** and **11b**, respectively, are in reasonable agreement with the corresponding motionally averaged values found in a $CDCl_3$ solution,[143] as well as the $^1J(^{77}Se,^{31}P)_{iso}$ values obtained from a solid-state phosphorus-31 NMR investigation.[144]

The values of δ_{ii} (calc.) for **11a** and **11b** are compared with the experimentally determined values in Table 2. The relatively accurate values of Ω (calc.) by all methods result from the lack of overestimation for the values of δ_{11} (calc.) as generally observed for the chemical shift tensors calculated in this investigation. The orientations calculated for compound **11** are the only ones investigated in this study that display significant differences between the two selenium environments **11a** and **11b**. All DFT calculations indicate that the selenium chemical shift tensor for **11a** is oriented such that δ_{11} is perpendicular to the Se−P vector and that this vector bisects the δ_{22}−Se−δ_{33} angle. While similar to that determined for **11a**, δ_{22} for **11b** is perpendicular to the Se−P bond, and it is the δ_{11}−Se−δ_{33} angle that is bisected by the bond vector. As for **11a**, the calculated orientations for **11b** are consistent regardless of the level of theory employed.

12. The calculated and experimental spectra obtained for tri-*para*-tolylphosphine selenide (*p*-Tol$_3$PSe) under MAS conditions are given in Figure 11. A spectrum of a stationary sample was not recorded. The experimental values of δ_{iso}, −242 ppm, and $^1J(^{77}Se,^{31}P)_{iso}$, −732 Hz, compare well with the corresponding solution ^{77}Se NMR values previously reported.[145] The principal components of the chemical shift tensor for **12** are reported in Table 2.

The calculated chemical shift tensor for selenium in *p*-Tol$_3$-PSe was obtained with the NR, SC, and SO calculations. The value of δ_{iso} (expt.) is well reproduced, and the individual principal components achieve slightly poorer agreement by all methods, as expected. Each of the calculations arrives at similarly oriented selenium chemical shift tensors. The Se−P vector is directed perpendicular to δ_{11} and bisects the δ_{22}−Se−δ_{33} angle (inset Figure 11). Despite structural similarities with **10**, the orientation of the chemical shift tensor PAS for **12** is different; however, orientations can differ when relatively small spans are encountered.

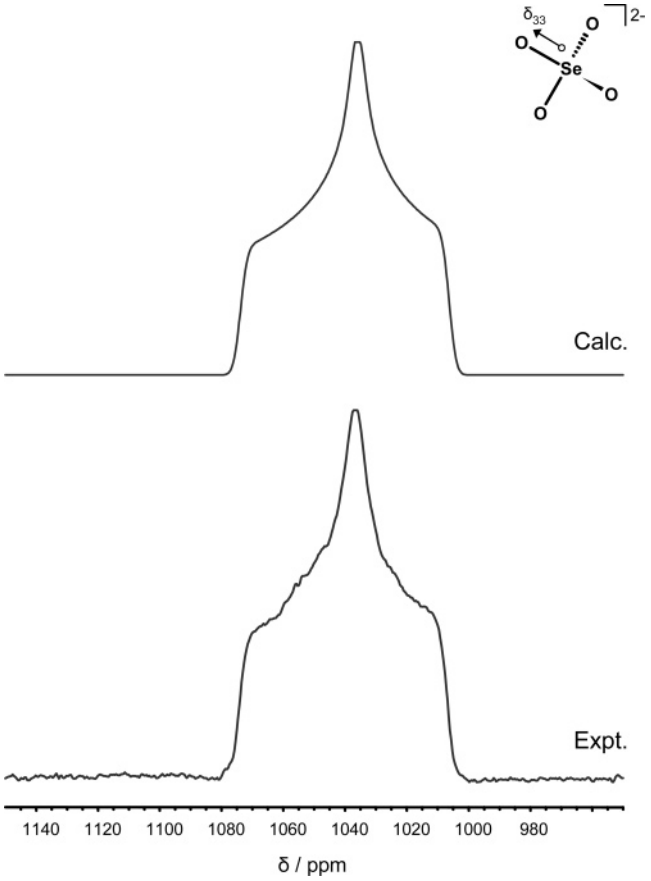

Figure 13. CP static ^{77}Se NMR and calculated spectra for $(NH_4)_2SeO_4$ (**14**) acquired at 9.4 T, requiring 188 transients, 100 Hz of line broadening, a contact time of 10.0 ms, and a recycle delay of 4 s. Inset is a schematic of compound **14** showing the orientation of the selenium chemical shift tensor calculated at the scalar with spin−orbit relativistic level of theory.

13. The experimental and simulated spectra for tris-2,4,6-trimethoxyphenylphosphine selenide (TTMPSe) are given in Figure 12. A spectrum for stationary **13** was not acquired. The principal components of the chemical shift tensor of **13** are given in Table 2. The span of the tensor is the largest observed of the organophosphine selenides investigated. The isotropic chemical shift, −30 ppm, and indirect spin−spin coupling constant, −735 Hz, are in excellent agreement with previously reported solution ^{77}Se NMR values.[145]

It is apparent from Table 2 that the NR and SC calculations have the greatest difficulty in reproducing the experimental value of δ_{33}. However, the SO calculation accurately reproduces the experimental value of δ_{33} and subsequently reproduces the entire chemical shift tensor for selenium to a greater extent in **13**. This improvement in calculating the entire chemical shift tensor is reflected in a more accurate value of Ω (calc.) with respect to Ω (expt.) (Table 2); however, the origin of the spin−orbit coupling effect for **13** is unclear in relation to the apparent lack of such a contribution for compounds **7**−**12**. All levels of theory predict that δ_{33} lies closest to the P−Se bond, as depicted inset in Figure 12.

Upon review of compounds **7**−**13**, it is apparent that even minor peripheral modifications to the phosphine selenide functional group can produce differences in the magnitude and orientation of the principal components of the selenium chemical shift tensor. All of the selenium chemical shift tensor principal components for the organophosphine selenides investigated show relatively small deshieldings along the direction of the P−Se bond indicating that the bonding environment is most appropriately described by a polarized, $R_3P^+-Se^-$, representation. In general the computations perform well regardless of the level of inclusion of relativistic effects.

TABLE 3: Experimental and Theoretical Chemical Shift Tensors[a] for Inorganic Selenium Compounds

	δ_{iso}	δ_{11}	δ_{22}	δ_{33}	Ω
14					
expt.[b]	1040.2	1076	1038	1008	68
expt.[c]	1040.2	1074.8	1037.8	1008.0	66.8
NR	941	973	959	891	82
SC	952	985	973	899	86
SO	981	1015	1001	928	87
15a					
expt.[b]	1338	1815	1787	412	1403
NR	1742	2306	1567	1353	953
SC	1430	2092	1488	710	1382
SO	1367	2030	1468	602	1428
15b					
expt.[b]	1256	1842	1561	364	1478
NR	1525	2049	1533	992	1057
SC	1254	1882	1423	456	1426
SO	1188	1808	1410	347	1461
15c					
expt.[b]	1155	1591	1584	291	1300
NR	1449	2016	1177	1153	863
SC	1204	1866	1107	638	1228
SO	1139	1793	1114	509	1284
16					
expt.[d]	2572.3				
NR	2789	4273	3951	142	4131
SC	2828	4331	4045	108	4223
SO	2817	4254	4204	-8	4262

[a] Chemical shifts in ppm with respect to external Me_2Se. [b] This work. [c] Reference 73. [d] Reference 147.

(3) Inorganic Selenium Compounds. While selenium will likely find itself in as many, if not more, different inorganic molecular environments as found in organoselenium compounds, the most likely to occur include selenium in a highly coordinated environment, selenium as a terminal moiety, and selenium as a bridging nucleus between inorganic nuclei. Thus, we investigated compounds **14**−**16** as representative examples.

14. Selenate anions are common oxidation products obtained in selenium chemistry. Figure 13 shows the ^{77}Se NMR spectrum of stationary $(NH_4)_2SeO_4$, along with its simulation. The principal components of the chemical shift tensor are compared with the earlier values of Collins et al.[73] in Table 3. The agreement is excellent for all components noting that as ammonium selenate was employed as the secondary reference, its isotropic shift was set to that reported previously, and perfect agreement in δ_{iso} is obviously achieved.[73]

The agreement between the calculated and experimental chemical shift tensors results in well-reproduced values of δ_{iso} and Ω (Table 3). The orientations calculated by all of the theoretical methods employed agree in their determination and that δ_{33} is parallel with a Se−O vector, as shown inset within Figure 13.

15. Selenotungstates have recently been utilized as selenium transfer agents in the preparation of organic diselenides.[146] The calculated and experimental spectra for $(NH_4)_2WSe_4$ are given in Figure 14. The tungsten sits on a mirror plane that contains two of the selenium atoms.[103] This yields three distinct chemical shift tensors for the four selenium atoms, whose principal components are given in Table 3, where **15a** corresponds to the two crystallographically equivalent selenium atoms. All of the chemical shift tensors for the selenium nuclei of $(NH_4)_2$-

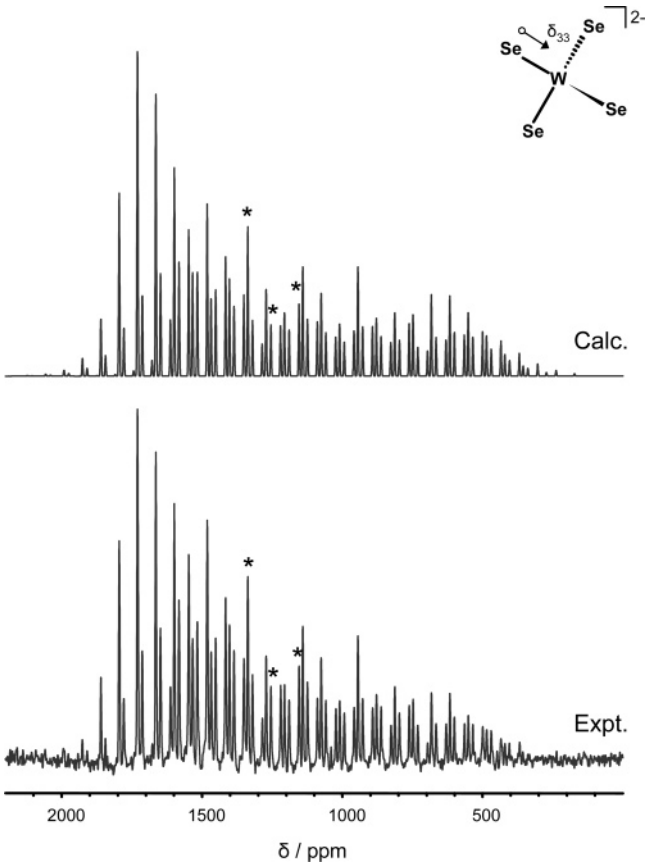

Figure 14. Experimental ^{77}Se CPMAS and simulated spectra for $(NH_4)_2WSe_4$ (**15**). Experimental conditions at 9.4 T: 1868 scans, ν_{rot} = 5.0 kHz, line broadened by 200 Hz, a contact time of 15.0 ms, and a 16 s pulse delay. Isotropic peaks are labeled with asterisks (*). Inset is a schematic of compound **15** showing the orientation of the selenium chemical shift tensor calculated at the scalar with spin−orbit relativistic level of theory.

WSe_4 have very large spans, and **15b** has the largest experimental span observed for all of the compounds investigated in this study.

Several distinctions occur for compound **15** from the general observations in the calculations of the chemical shift tensors for the majority of the compounds investigated herein. While the δ_{11} (calc.) values from all three methods for **15a** and **15c** overestimate the corresponding experimental values, the calculations do not underestimate δ_{33}. The nonrelativistic calculations for all three chemical shift tensors for **15** significantly overestimate the value of δ_{33} (Table 3). Both relativistic calculations come much closer to reproducing δ_{33} (expt.), and as a consequence of this achieve more accurate values of the span than the NR calculations (Table 3 and Figure 4). Thus, a significant difference between the computation methods employed on the compounds investigated in this study occurs between the nonrelativistic and the two relativistic calculations for all of the chemical shift tensors for **15**. All levels of theory indicate that the orientation of the chemical shift tensors for **15a**, **15b**, and **15c** are such that the direction of δ_{33} is directed along the Se−W vector (inset Figure 14).

16. The molecular environment within $[CpCr(CO)_2]_2Se$ possesses a bridging selenium between the two chromium centers. Such an environment, similar to the organic dialkyl selenides, can be found commonly in inorganic selenium compounds. Unfortunately, we were unable to characterize the selenium chemical shift tensor of this compound experimentally. Given the accuracy and predictive capability of the DFT calculations in the previous compounds investigated, the magnetic shielding tensor was calculated. The crystal structure of this compound has previously been reported and indicates the presence of a single selenium atom in the asymmetric unit.[104] Thus, only one magnetic shielding tensor was calculated, and the isotropic shift of the corresponding chemical shift tensor could then be compared with a solution value determined by Dean and co-workers (see Table 3).[147] The calculated values of δ_{11} and δ_{22} are approximately of the same magnitude and are extremely deshielded with respect to the reference. The δ_{33} (calc.) direction is significantly more shielded than the previous two principal components. The large difference between δ_{11} and δ_{33} yields a tensor with the largest value of Ω calculated in this study. The large span may be the cause of the difficulty in observing the chemical shift tensor experimentally. Because of the lack of experimental values of δ_{ii}, the only point of comparison available is with the solution value of δ_{iso}. The large deshielded isotropic resonance observed experimentally is adequately reproduced considering the potential of solvent effects and solid-to-solution shifts that may affect the bridging selenium in this compound. The calculated orientation of the chemical shift tensors are in agreement, regardless of the method employed, and δ_{33} is parallel with the approximately linear Cr−Se−Cr vector. The plane normal to this vector containing the selenium is composed by the two extremely deshielded components, δ_{11} and δ_{22}.

Summary

Selenium chemical shift tensors for a wide variety of compounds were investigated representing the entire known isotropic chemical shift range of selenium. ZORA DFT calculations complement the experimental work and suggest that the orientation of the selenium chemical shift tensor is not only sensitive to what is directly bonded to the selenium atom but also to the next nearest neighbors and beyond. The calculations were carried out with varying degrees of relativistic corrections applied in an effort to assess the importance of relativistic effects. Isotropic chemical shifts were found to be calculated approximately equally well by all methods. Generally, the values of δ_{33} were underestimated by the calculations, and coupled with the overestimations obtained for δ_{11} (calc.), overestimated calculated spans often resulted. The large underestimation of Ω(NR) for $(NH_4)_2WSe_4$ is unique out of all of the spans obtained. This results from the failure of the NR calculation to reproduce δ_{33} (expt.), noting that the direction of this principal component is predicted by the calculations to coincide with the direction of the Se−W bond. Tungsten is the heaviest element (Z = 74) in all of the compounds investigated, and it is not surprising that relativistic calculations are required to properly describe the magnetic shielding interaction for selenium in ammonium selenotungstate. Considering all of the selenium chemical shift tensors investigated in this study, the scalar with spin−orbit relativistic calculations generally performed better, if only slightly, than the nonrelativistic and scalar relativistic calculations. The size of a given selenium-containing system will determine whether the additional computational time required for the relativistic calculations is feasible. Should the selenium atom find itself bonded to a heavier element, such as tungsten, the need for the inclusion of relativistic effects becomes warranted.

Acknowledgment. We thank the Natural Sciences and Engineering Research Council of Canada, the Alberta Ingenuity Fund, and the University of Alberta for research grants and scholar-

ships. R.E.W. is a Canada Research Chair in Physical Chemistry at the University of Alberta. The authors wish to thank Professor Glenn H. Penner for preparing the trimethylphosphine selenide and tris-(*tert*-butyl)phosphine selenide, Professor Gang Wu for some preliminary experiments on ammonium selenotungstate, and Professor P. -N. Roy for generous use of some computing resources.

Supporting Information Available: The linear regression parameters, slope and intercept, along with the mean absolute deviation for the plots in Figures 2−4 have been tabulated. This material is available free of charge via the Internet at http://pubs.acs.org.

References and Notes

(1) Alivisatos, A. P. *Science* **1996**, *271*, 933.
(2) Xu, R.; Husmann, A.; Rosenbaum, T. F.; Saboungi, M.-L.; Enderby, J. E.; Littlewood, P. B. *Nature (London)* **1997**, *390*, 57.
(3) Johnson, J. A.; Saboungi, M.-L.; Thiyagarajan, P.; Csencsits, R.; Meisel, D. *J. Phys. Chem. B* **1999**, *103*, 59.
(4) Mayers, B.; Jiang, X.; Sunderland, D.; Cattle, B.; Xia, Y. *J. Am. Chem. Soc.* **2003**, *125*, 13364.
(5) Terasaki, O.; Yamazaki, K.; Thomas, J. M.; Ohsuna, T.; Watanabe, D.; Sanders, J. V.; Barry, J. C. *Nature (London)* **1987**, *330*, 58.
(6) Endo, H.; Inui, M.; Yao, M.; Tamura, K.; Hoshino, H.; Katayama, Y.; Maruyama, K. *Z. Phys. Chem. Neue Folge* **1988**, *156*, 507.
(7) Parise, J. B.; MacDougall, J. E.; Herron, N.; Farlee, R.; Sleight, A. W.; Wang, Y.; Bein, T.; Moller, K.; Moroney, L. M. *Inorg. Chem.* **1988**, *27*, 221.
(8) Nozue, Y.; Kodaira, T.; Terasaki, O.; Yamazaki, K.; Goto, T.; Watanabe, D.; Thomas, J. M. *J. Phys.: Condens. Matter* **1990**, *2*, 5209.
(9) Goldbach, A.; Iton, L. E.; Saboungi, M.-L. *Chem. Phys. Lett.* **1997**, *281*, 69.
(10) Goldbach, A.; Saboungi, M.-L. *Acc. Chem. Res.* **2005**, *38*, 705.
(11) Oldfield, J. E. *J. Nutr.* **1987**, *117*, 2002.
(12) Böck, A.; Forchhammer, K.; Heider, J.; Leinfelder, W.; Sawers, G.; Veprek, B.; Zinoni, F. *Mol. Microbiol.* **1991**, *5*, 515.
(13) Salzmann, M.; Stocking, E. M.; Silks III, L. A.; Senn, H. *Magn. Reson. Chem.* **1999**, *37*, 672.
(14) Mikulec, F. V.; Kuno, M.; Bennati, M.; Hall, D. A.; Griffin, R. G.; Bawendi, M. G. *J. Am. Chem. Soc.* **2000**, *122*, 2532.
(15) Liu, Y.; Li, L.; Fan, Z.; Zhang, H.-Y.; Wu, X.; Guan, X.-D.; Liu, S.-X. *Nano Lett.* **2002**, *2*, 257.
(16) Zelakiewicz, B. S.; Yonezawa, T.; Tong, Y.-Y. *J. Am. Chem. Soc.* **2004**, *126*, 8112.
(17) Berrettini, M. G.; Braun, G.; Hu, J. G.; Strouse, G. F. *J. Am. Chem. Soc.* **2004**, *126*, 7063.
(18) Duddeck, H. *Prog. Nucl. Magn. Reson. Spectrosc.* **1995**, *27*, 1.
(19) Duddeck, H. *Annu. Rep. NMR Spectrosc.* **2004**, *52*, 105.
(20) Pulay, P. In *Calculation of NMR and EPR Parameters*; Kaupp, M., Bühl, M., Malkin, V. G., Eds.; Wiley-VCH Verlag GmbH & Co. KGaA: Weinheim, Germany, 2004; pp XIII.
(21) McFarlane, H. C. E.; McFarlane, W. Selenium-77 and Tellurium-125. In *NMR of Newly Accessible Nuclei*; Laszlo, P., Ed.; Academic Press: New York, 1983; Vol. 2, p 275.
(22) Luthra, N. P.; Odom, J. D. Nuclear Magnetic Resonance and Electron Spin Resonance Studies of Organic Selenium and Tellurium Compounds. In *The Chemistry of Organic Selenium and Tellurium Compounds*; Patai, S., Rappoport, Z., Eds.; John Wiley & Sons: New York, 1986; Vol. 1, p 189.
(23) McFarlane, H. C. E.; McFarlane, W. Sulfur, Selenium, and Tellurium. In *Multinuclear NMR*; Mason, J., Ed.; Plenum Press: New York, 1987; p 417.
(24) Klapötke, T. M.; Broschag, M. *Compilation of Reported ^{77}Se NMR Chemical Shifts: Up to the Year 1994*; Wiley: Chichester, U.K., 1996.
(25) Sefzik, T. H.; Turco, D.; Iuliucci, R. J.; Facelli, J. C. *J. Phys. Chem. A* **2005**, *109*, 1180.
(26) Veeman, W. S. *Philos. Trans. R. Soc. London, Ser. A* **1981**, *299*, 629.
(27) Grossmann, G.; Potrzebowski, M. J.; Fleischer, U.; Krüger, K.; Malkina, O. L.; Ciesielski, W. *Solid State Nucl. Magn. Reson.* **1998**, *13*, 71.
(28) Yates, J. R.; Pickard, C. J.; Payne, M. C.; Mauri, F. *J. Chem. Phys.* **2003**, *118*, 5746.
(29) Tossell, J. A.; Lazzeretti, P. *J. Magn. Reson.* **1988**, *80*, 39.
(30) Magyarfalvi, G.; Pulay, P. *Chem. Phys. Lett.* **1994**, *225*, 280.
(31) Bühl, M.; Thiel, W.; Fleischer, U.; Kutzelnigg, W. *J. Phys. Chem.* **1995**, *99*, 4000.
(32) Schreckenbach, G.; Ruiz-Morales, Y.; Ziegler, T. *J. Chem. Phys.* **1996**, *104*, 8605.
(33) Nakanishi, W.; Hayashi, S. *Chem. Lett.* **1998**, 523.
(34) Hayashi, S.; Nakanishi, W. *J. Org. Chem.* **1999**, *64*, 6688.
(35) Bernard, G. M.; Eichele, K.; Wu, G.; Kirby, C. W.; Wasylishen, R. E. *Can. J. Chem.* **2000**, *78*, 614.
(36) Campbell, J.; Mercier, H. P. A.; Santry, D. P.; Suontamo, R. J.; Borrmann, H.; Schrobilgen, G. J. *Inorg. Chem.* **2001**, *40*, 233.
(37) Tattershall, B. W.; Sandham, E. L. *J. Chem. Soc., Dalton Trans.* **2001**, 1834.
(38) Wilson, P. J. *Mol. Phys.* **2001**, *99*, 363.
(39) Bayse, C. A. *Inorg. Chem.* **2004**, *43*, 1208.
(40) Chesnut, D. B. *Chem. Phys.* **2004**, *305*, 237.
(41) Bayse, C. A. *J. Chem. Theory Comput.* **2005**, *1*, 1119.
(42) Chang, C.; Pelissier, M.; Durand, P. *Phys. Scr.* **1986**, *34*, 394.
(43) van Lenthe, E.; Baerends, E. J.; Snijders, J. G. *J. Chem. Phys.* **1993**, *99*, 4597.
(44) van Lenthe, E.; Baerends, E. J.; Snijders, J. G. *J. Chem. Phys.* **1994**, *101*, 9783.
(45) van Lenthe, E.; van Leeuwen, R.; Baerends, E. J.; Snijders, J. G. *Int. J. Quantum Chem.* **1996**, *57*, 281.
(46) Kennedy, M. A.; Ellis, P. D. *Concepts Magn. Reson.* **1989**, *1*, 35.
(47) Kennedy, M. A.; Ellis, P. D. *Concepts Magn. Reson.* **1989**, *1*, 109.
(48) Power, W. P.; Mooibroek, S.; Wasylishen, R. E.; Cameron, T. S. *J. Phys. Chem.* **1994**, *98*, 1552.
(49) Eichele, K.; Wu, G.; Wasylishen, R. E.; Britten, J. F. *J. Phys. Chem.* **1995**, *99*, 1030.
(50) Eichele, K.; Wasylishen, R. E.; Corrigan, J. F.; Taylor, N. J.; Carty, A. J.; Feindel, K. W.; Bernard, G. M. *J. Am. Chem. Soc.* **2002**, *124*, 1541.
(51) Ramsey, N. F. *Molecular Beams*; Oxford University Press: London, 1956.
(52) Ramsey, N. F. *Phys. Rev.* **1950**, *78*, 699.
(53) Pyykkö, P. *Theor. Chem. Acc.* **2000**, *103*, 214.
(54) Pyper, N. C. *Chem. Phys. Lett.* **1983**, *96*, 204.
(55) Pyper, N. C. *Chem. Phys. Lett.* **1983**, *96*, 211.
(56) Pyykkö, P. *Chem. Phys.* **1983**, *74*, 1.
(57) Zhang, Z. C.; Webb, G. A. *J. Mol. Struct.* **1983**, *104*, 439.
(58) Kolb, D.; Johnson, W. R.; Shorer, P. *Phys. Rev. A* **1982**, *26*, 19.
(59) Kutzelnigg, W. *J. Comput. Chem.* **1999**, *20*, 1199.
(60) Vaara, J.; Malkina, O. L.; Stoll, H.; Malkin, V. G.; Kaupp, M. *J. Chem. Phys.* **2001**, *114*, 61.
(61) Autschbach, J.; Ziegler, T. Relativistic Computation of NMR Shieldings and Spin-Spin Coupling Constants. In *Encyclopedia of Nuclear Magnetic Resonance*; Grant, D. M., Harris, R. K., Eds.; John Wiley and Sons, Ltd.: Chichester, U.K., 2002; Vol. 9, p 306.
(62) Manninen, P.; Lantto, P.; Vaara, J.; Ruud, K. *J. Chem. Phys.* **2003**, *119*, 2623.
(63) Pyykkö, P. Theory of NMR parameters. From Ramsey to Relativity, 1953 to 1983. In *Calculation of NMR and EPR Parameters*; Kaupp, M., Bühl, M., Malkin, V. G., Eds.; Wiley-VCH Verlag GmbH & Co. KGaA: Weinheim, Germany, 2004; p 7.
(64) Ramsey, N. F. *Phys. Rev.* **1953**, *91*, 303.
(65) Jameson, C. J. Spin-Spin Coupling. In *Multinuclear NMR*; Mason, J., Ed.; Plenum Press: New York, 1987; p 89.
(66) Fukui, H. *Prog. Nucl. Magn. Reson. Spectrosc.* **1999**, *35*, 267.
(67) Contreras, R. H.; Peralta, J. E.; Giribet, C. G.; De Azua, M. C.; Facelli, J. C. *Annu. Rep. NMR Spectrosc.* **2000**, *41*, 55.
(68) Vaara, J.; Jokisaari, J.; Wasylishen, R. E.; Bryce, D. L. *Prog. Nucl. Magn. Reson. Spectrosc.* **2002**, *41*, 233.
(69) Wasylishen, R. E. Dipolar & Indirect Coupling Tensors in Solids. In *Encyclopedia of Nuclear Magnetic Resonance*; Grant, D. M.; Harris, R. K., Eds.; John Wiley and Sons: Ltd.: Chichester, U.K., 2002; Vol. 9, p 1685.
(70) Jameson, C. J. Theoretical Considerations: Spin-Spin Coupling. In *Phosphorus-31 NMR Spectroscopy in Stereochemical Analysis. Organic Compounds and Metal Complexes*; Verkade, J. G., Quin, L. D., Eds.; VCH Publishers: Deerfield Beach, 1987; p 205.
(71) Eichele, K.; Wasylishen, R. E. *J. Magn. Reson., Ser. A* **1994**, *106*, 46.
(72) Nicpon, P.; Meek, D. W. *Inorg. Synth.* **1967**, *10*, 157.
(73) Collins, M. J.; Ratcliffe, C. I.; Ripmeester, J. A. *J. Magn. Reson.* **1986**, *68*, 172.
(74) Bryce, D. L.; Bernard, G. M.; Gee, M.; Lumsden, M. D.; Eichele, K.; Wasylishen, R. E. *Can. J. Anal. Sci. Spectrosc.* **2001**, *46*, 46.
(75) Herzfeld, J.; Berger, A. E. *J. Chem. Phys.* **1980**, *73*, 6021.
(76) Eichele, K.; Wasylishen, R. E. *WSOLIDS NMR Simulation Package*, 1.17.30 ed.; 2001.
(77) Schreckenbach, G.; Ziegler, T. *J. Phys. Chem.* **1995**, *99*, 606.
(78) Schreckenbach, G.; Ziegler, T. *Int. J. Quantum Chem.* **1997**, *61*, 899.
(79) Wolff, S. K.; Ziegler, T. *J. Chem. Phys.* **1998**, *109*, 895.
(80) *ADF 2004.01 Theoretical Chemistry*; Vrije Universiteit: Amsterdam; http://www.scm.com.
(81) Baerends, E. J.; Ellis, D. E.; Ros, P. *Chem. Phys.* **1973**, *2*, 41.

(82) Versluis, L.; Ziegler, T. *J. Chem. Phys.* **1988**, *88*, 322.
(83) te Velde, G.; Baerends, E. J. *J. Comput. Phys.* **1992**, *99*, 84.
(84) Fonseca Guerra, C.; Snijders, J. G.; te Velde, G.; Baerends, E. J. *Theor. Chem. Acc.* **1998**, *99*, 391.
(85) Vosko, S. H.; Wilk, L.; Nusair, M. *Can. J. Phys.* **1980**, *58*, 1200.
(86) Becke, A. D. *Phys. Rev. A* **1988**, *38*, 3098.
(87) Perdew, J. P. *Phys. Rev. B* **1986**, *33*, 8822.
(88) Perdew, J. P. *Phys. Rev. B* **1986**, *34*, 7406.
(89) Pathirana, H. M. K. K.; Weiss, T. J.; Reibenspies, J. H.; Zingaro, R. A.; Meyers, E. A. *Z. Kristallogr.* **1994**, *209*, 697.
(90) Husebye, S.; Lindeman, S. V.; Rudd, M. D. *Acta Crystallogr., Sect. C: Cryst. Struct. Commun.* **1997**, *53*, 809.
(91) McCullough, J. D.; Hamburger, G. *J. Am. Chem. Soc.* **1942**, *64*, 508.
(92) Rajeswaran, M.; Parthasarathy, R. *Acta Crystallogr., Sect. C: Cryst. Struct. Commun.* **1984**, *40*, 647.
(93) Kistenmacher, T. J.; Emge, T. J.; Shu, P.; Cowan, D. O. *Acta Crystallogr., Sect. B: Struct. Sci.* **1979**, *35*, 772.
(94) Marsh, R. E. *Acta Crystallogr.* **1952**, *5*, 458.
(95) Cogne, A.; Grand, A.; Laugier, J.; Robert, J. B.; Wiesenfeld, L. *J. Am. Chem. Soc.* **1980**, *102*, 2238.
(96) Steinberger, H.-U.; Ziemer, B.; Meisel, M. *Acta Crystallogr., Sect. C: Cryst. Struct. Commun.* **2001**, *57*, 323.
(97) Davies, J. A.; Dutremez, S.; Pinkerton, A. A. *Inorg. Chem.* **1991**, *30*, 2380.
(98) Jones, P. G.; Kienitz, C.; Thone, C. *Z. Kristallogr.* **1994**, *209*, 80.
(99) Alyea, E. C.; Ferguson, G.; Malito, J.; Ruhl, B. L. *Acta Crystallogr., Sect. C: Cryst. Struct. Commun.* **1986**, *42*, 882.
(100) Zhdanov, G. S.; Pospelov, V. A.; Umanskii, M. M.; Glushkova, V. P. *Dokl. Akad. Nauk SSSR* **1953**, *92*, 983.
(101) Allen, D. W.; Bell, N. A.; March, L. A.; Nowell, I. W. *Polyhedron* **1990**, *9*, 681.
(102) Carter, R. L.; Koerntgen, C.; Margulis, T. N. *Acta Crystallogr., Sect. B: Struct. Sci.* **1977**, *33*, 592.
(103) Müller, A.; Krebs, B.; Beyer, H. *Z. Naturforsch.* **1968**, *23B*, 1537.
(104) Goh, L. Y.; Wei, C.; Sinn, E. *Chem. Commun.* **1985**, 462.
(105) Valeev, R. B.; Kalabin, G. A.; Kushnarev, D. F. *Zh. Org. Khim.* **1980**, *16*, 2482.
(106) Luthra, N. P.; Dunlap, R. B.; Odom, J. D. *J. Magn. Reson.* **1983**, *52*, 318.
(107) Carr, S. W.; Colton, R. *Aust. J. Chem.* **1981**, *34*, 35.
(108) Facey, G.; Wasylishen, R. E.; Collins, M. J.; Ratcliffe, C. I.; Ripmeester, J. A. *J. Phys. Chem.* **1986**, *90*, 2047.
(109) Jameson, C. J.; Jameson, A. K. *Chem. Phys. Lett.* **1987**, *135*, 254.
(110) Bühl, M.; Gauss, J.; Stanton, J. F. *Chem. Phys. Lett.* **1995**, *241*, 248.
(111) Balzer, G.; Duddeck, H.; Fleischer, U.; Röhr, F. *Fresenius' J. Anal. Chem.* **1997**, *357*, 473.
(112) Nakanishi, W.; Hayashi, S. *J. Phys. Chem. A* **1999**, *103*, 6074.
(113) Odom, J. D.; Dawson, W. H.; Ellis, P. D. *J. Am. Chem. Soc.* **1979**, *101*, 5815.
(114) Dong, S.; Ida, R.; Wu, G. *J. Phys. Chem. A* **2000**, *104*, 11194.
(115) Wong, T. C.; Ang, T. T.; Guziec, F. S.; Moustakis, C. A. *J. Magn. Reson.* **1984**, *57*, 463.
(116) Dong, S.; Yamada, K.; Wu, G. *Z. Naturforsch., A* **2000**, *55*, 21.
(117) Opella, S. J.; Frey, M. H.; Cross, T. A. *J. Am. Chem. Soc.* **1979**, *101*, 5856.
(118) Zumbulyadis, N.; Henrichs, P. M.; Young, R. H. *J. Chem. Phys.* **1981**, *75*, 1603.
(119) Hexem, J. G.; Frey, M. H.; Opella, S. J. *J. Chem. Phys.* **1982**, *77*, 3847.
(120) Menger, E. M.; Veeman, W. S. *J. Magn. Reson.* **1982**, *46*, 257.
(121) Böhm, J.; Fenzke, D.; Pfeifer, H. *J. Magn. Reson.* **1983**, *55*, 197.
(122) Olivieri, A. C.; Frydman, L.; Diaz, L. E. *J. Magn. Reson.* **1987**, *75*, 50.
(123) Alarcón, S. H.; Olivieri, A. C.; Harris, R. K. *Solid State Nucl. Magn. Reson.* **1993**, *2*, 325.
(124) Grondona, P.; Olivieri, A. C. *Concepts Magn. Reson.* **1993**, *5*, 319.
(125) Harris, R. K.; Olivieri, A. C. *Prog. Nucl. Magn. Reson. Spectrosc.* **1992**, *24*, 435.
(126) Saatsazov, V. V.; Khotsyanova, T. L.; Magdesieva, N. N.; Kuznetsov, S. I.; Alymov, I. M.; Kyandzhetsian, R. A.; Bryukhova, E. V. *Izv. Akad. Nauk SSSR, Ser. Khim.* **1974**, *12*, 2850.
(127) Saatsazov, V. V.; Khotsyanova, T. L.; Kazakov, V. P.; Bryukhova, E. V. *Izv. Akad. Nauk SSSR, Ser. Fiz.* **1975**, *39*, 2535.
(128) Collins, M. J.; Ripmeester, J. A. *J. Am. Chem. Soc.* **1987**, *109*, 4113.
(129) Clayden, N. J.; Dobson, C. M.; Lian, L.-Y.; Smith, D. J. *J. Magn. Reson.* **1986**, *69*, 476.
(130) Drabowicz, J.; Luczak, J.; Mikolajczyk, M. *J. Org. Chem.* **1998**, *63*, 9565.
(131) Potrzebowski, M. J.; Katarzyński, R.; Ciesielski, W. *Magn. Reson. Chem.* **1999**, *37*, 173.
(132) Batchelor, R. J.; Einstein, F. W. B.; Gay, I. D.; Gu, J.-H.; Pinto, B. M.; Zhou, X.-M. *Can. J. Chem.* **2000**, *78*, 598.
(133) Frère, P.; Skabara, P. J. *Chem. Soc. Rev.* **2005**, *34*, 69.
(134) Duddeck, H.; Bradenahl, R.; Stefaniak, L.; Jazwinski, J.; Kamienski, B. *Magn. Reson. Chem.* **2001**, *39*, 709.
(135) Jacques-Silva, M. C.; Nogueira, C. W.; Broch, L. C.; Flores, É. M. M.; Rocha, J. B. T. *Pharmacol. Toxicol.* **2001**, *88*, 119.
(136) Rossato, J. I.; Ketzer, L. A.; Centurião, F. B.; Silva, S. J. N.; Lüdtke, D. S.; Zeni, G.; Braga, A. L.; Rubin, M. A.; Rocha, J. B. T. *Neurochem. Res.* **2002**, *27*, 297.
(137) Maciel, E. N.; Flores, É. M. M.; Rocha, J. B. T.; Folmer, V. *Bull. Environ. Contam. Toxicol.* **2003**, *70*, 470.
(138) Wirth, T. *Molecules* **1998**, *3*, 164.
(139) Wilson, S. R.; Zucker, P. A.; Huang, R.-R. C.; Spector, A. *J. Am. Chem. Soc.* **1989**, *111*, 5936.
(140) du Mont, W.-W. *Z. Naturforsch.* **1985**, *40B*, 1453.
(141) Rajalingam, U.; Dean, P. A. W.; Jenkins, H. A. *Can. J. Chem.* **2000**, *78*, 590.
(142) Bryce, D. L.; Eichele, K.; Wasylishen, R. E. *Inorg. Chem.* **2003**, *42*, 5085.
(143) Allen, D. W.; Taylor, B. F. *J. Chem. Res.-S* **1986**, 392.
(144) Eichele, K.; Wasylishen, R. E.; Kessler, J. M.; Solujić, L.; Nelson, J. H. *Inorg. Chem.* **1996**, *35*, 3904.
(145) Allen, D. W.; Nowell, I. W.; Taylor, B. F. *J. Chem. Soc., Dalton Trans.* **1985**, 2505.
(146) Saravanan, V.; Porhiel, E.; Chandrasekaran, S. *Tetrahedron Lett.* **2003**, *44*, 2257.
(147) Dean, P. A. W.; Goh, L. Y.; Gay, I. D.; Sharma, R. D. *J. Organomet. Chem.* **1997**, *533*, 1.